Available online at www.eccomasproceedia.org
Eccomas Proceedia SMART (2023) 1-10

ECCOMAS
Proceedia

X ECCOMAS Thematic Conference on Smart Structures and Materials
SMART 2023
D.A. Saravanos, A. Benjeddou, N. Chrysochoidis and T. Theodosiou (Eds)

IMPLICATIONS OF CRACK FACE CONDITIONS IN FRACTURE MECHANICS OF DIELECTRICS EMANATING FROM CLOSED FORM SOLUTIONS

LENNART BEHLEN*, DANIEL WALLENTA† AND ANDREAS RICOEUR*

*Institute of Mechanics
University of Kassel, 34125 Kassel, Germany
e-mail: behlen@uni-kassel.de

†Institute of Mathematics
University of Kassel, 34109 Kassel, Germany

Abstract. Fracture mechanics of dielectrics is particurlarly concerned with the impact of electric fields on crack tip loading, and thus with appropriate electric and mechanical boundary conditions at the crack faces. To this end, the so-called capacitor analogy provides approximate surface charges and Coulombic tractions on the boundaries, the latter of which represent a simplification of the true Maxwell surface tractions, without solving two-domain problems of bulk material and crack interior. In this work, the quality of these approximations is assessed by means of the analytic solution of an elliptic cavity in an infinite dielectric satisfying the exact interface conditions at the ellipse. As turns out, the surface charges represent an excellent substitute for the exact electric boundary conditions within a broad range of parameters, whereas the large errors of the Coulombic tractions near the crack tip due to curvature lead to a significantly underestimated mode I stress intensity factor.

Key words: smart materials, dielectrics, Maxwell stress, crack boundary conditions, Griffith crack

1 INTRODUCTION

Aside from mechanical stresses, dielectric ceramics may be subjected to electric fields for the purpose of multifunctional applications, in particular with regard to piezoelectrics. Consequently, fracture analysis of these brittle materials must account for the influence of electric fields on the loading situation at the crack tip. In light of this, the appropriate choice of electric boundary conditions on the crack faces is of utmost importance. Accounting for the electric permeability of a mechanically distorted crack without solving coupled two-domain problems with electric interface conditions of bulk material and crack medium, the so-called capacitor analogy developed by Hao and Shen [1] treats each two opposite points on the opened upper and lower crack faces S_c^+ and S_c^- as one-dimensional plate capacitor, enabling the employment

Peer-review under responsibility of the organizing committee of SMART 2023.
doi: 10.7712/150123.9759.444511

of approximated surface charge densities $\omega_\mathrm{S}^\mathrm{C}$ on the boundaries as functions of the unknown voltage and distance between both points, i.e.,

$$\omega_\mathrm{S}^\mathrm{C}(\mathbf{x}) = \begin{cases} -\kappa_\mathrm{C}\frac{\alpha(\mathbf{x}_\mathrm{c}^+(\mathbf{x}))-\alpha(\mathbf{x}_\mathrm{c}^-(\mathbf{x}))}{u_2(\mathbf{x}_\mathrm{c}^+(\mathbf{x}))-u_2(\mathbf{x}_\mathrm{c}^-(\mathbf{x}))}\,, & \mathbf{x}\in S_\mathrm{c}^+ \\ \kappa_\mathrm{C}\frac{\alpha(\mathbf{x}_\mathrm{c}^+(\mathbf{x}))-\alpha(\mathbf{x}_\mathrm{c}^-(\mathbf{x}))}{u_2(\mathbf{x}_\mathrm{c}^+(\mathbf{x}))-u_2(\mathbf{x}_\mathrm{c}^-(\mathbf{x}))}\,, & \mathbf{x}\in S_\mathrm{c}^- \end{cases}, \quad \mathbf{x}_\mathrm{c}^+\in S_\mathrm{c}^+\,, \mathbf{x}_\mathrm{c}^-\in S_\mathrm{c}^-\,, \tag{1}$$

where $\mathbf{x}$ denotes the position vector, κ_C is the permittivity of the crack medium, α is the electrostatic potential and u_2 is the displacement vertical to the crack plane. Accommodating the electrostatic energy of the crack medium, Landis [2] complemented the model by Coulombic tractions t_2^C acting on the crack faces, which emanate from the true Maxwell surface tractions $\mathbf{t}^\mathrm{M}$ under suitable simplifications [3], reading

$$t_2^\mathrm{C}(\mathbf{x}) = \begin{cases} -\frac{1}{2}\kappa_\mathrm{C}\left(\frac{\alpha(\mathbf{x}_\mathrm{c}^+(\mathbf{x}))-\alpha(\mathbf{x}_\mathrm{c}^-(\mathbf{x}))}{u_2(\mathbf{x}_\mathrm{c}^+(\mathbf{x}))-u_2(\mathbf{x}_\mathrm{c}^-(\mathbf{x}))}\right)^2, & \mathbf{x}\in S_\mathrm{c}^+ \\ \frac{1}{2}\kappa_\mathrm{C}\left(\frac{\alpha(\mathbf{x}_\mathrm{c}^+(\mathbf{x}))-\alpha(\mathbf{x}_\mathrm{c}^-(\mathbf{x}))}{u_2(\mathbf{x}_\mathrm{c}^+(\mathbf{x}))-u_2(\mathbf{x}_\mathrm{c}^-(\mathbf{x}))}\right)^2, & \mathbf{x}\in S_\mathrm{c}^- \end{cases}, \quad \mathbf{x}_\mathrm{c}^+\in S_\mathrm{c}^+\,, \mathbf{x}_\mathrm{c}^-\in S_\mathrm{c}^-\,. \tag{2}$$

While the quality of the capacitor analogy has been investigated numerically for inclined electric loads with regard to the approximated surface charges [4], a likewise assessment of the Coulombic tractions is still pending, in particular considering curvature of crack faces prevailing under load. In the following, the boundary value problem of an elliptic cavity in an infinite dielectric will be analyzed, as it provides a Griffith crack in the limiting case of $b \to 0$, whereas ellipses with $b > 0$ may serve as models for mechanically opened cracks.

2 THEORETICAL FRAMEWORK

Let a linear isotropic dielectric body with permittivity $\kappa^\mathrm{o} \geq \kappa_0$ occupy the infinite three-dimensional space minus an elliptic cylinder with semi-major and -minor axis a and b, respectively, of infinite height placed at the origin. The cylinder itself is filled with another linear isotropic dielectric or vacuum with permittivity $\kappa^\mathrm{i} \geq 0$. While the interior of both regions is governed by the electrostatic Maxwell equations in terms of Gauss' and Faraday's law in the absence of volume charges, the inner material boundary surface devoid of unbounded charge is subjected to the corresponding interface conditions requiring the continuity of tangential and normal components of the electric field and electric displacement, respectively. At infinity, a constant electric field is prescribed in the x_1-x_2-plane, which, considering the problem's symmetry, results in vanishing x_3-components and zero gradients of the electric field and displacement vectors along the x_3-axis. This allows for the reduction of the problem to two dimensions. Letting

$$\Omega^\mathrm{i} = \{\mathbf{x}\in\mathbb{R}^2 \mid (x_1/a)^2 + (x_2/b)^2 < 1\} \tag{3}$$

denote the set of all points lying inside the ellipse $\Gamma = \partial\Omega^\mathrm{i}$, and thus $\Omega^\mathrm{o} = \mathbb{R}^2 \setminus \overline{\Omega^\mathrm{i}}$ refer to the set of all points lying outside[1], the constitutive equation interlinking electric displacement

[1] a bar marks the set's closure.

$\mathbf{D}$ and electric field $\mathbf{E}$ reads:

$$\mathbf{D} = \begin{cases} \kappa^{\mathrm{o}}\mathbf{E} & \text{in } \Omega^{\mathrm{o}} \\ \kappa^{\mathrm{i}}\mathbf{E} & \text{in } \Omega^{\mathrm{i}} \end{cases} . \tag{4}$$

In conclusion, the following boundary value problem emerges: the vector fields $\mathbf{E}, \mathbf{D} \in C^1(\Omega^{\mathrm{i}} \cup \Omega^{\mathrm{o}}, \mathbb{R}^2)$ are sought, so that the field equations[2]

$$\begin{matrix} \operatorname{div} \mathbf{D} = 0 \\ \operatorname{curl} \mathbf{E} = 0 \end{matrix} \quad \text{in } \Omega^{\mathrm{i}} \cup \Omega^{\mathrm{o}} , \tag{5}$$

the interface conditions

$$\begin{matrix} [\![\mathbf{E}]\!] \cdot \mathbf{e}^{\mathrm{t}} = 0 \\ [\![\mathbf{D}]\!] \cdot \mathbf{e}^{\mathrm{n}} = 0 \end{matrix} \quad \text{on } \Gamma , \tag{6}$$

as well as the condition at infinity

$$\mathbf{E} = \mathbf{E}^{\infty} = \text{const} , \quad |\mathbf{x}| \to \infty \tag{7}$$

are satisfied. In Eqs. (6) and (7), Γ is parameterized counterclockwise and $\mathbf{e}^{\mathrm{t}}$ and $\mathbf{e}^{\mathrm{n}}$ represent unit vectors tangential and normal to Γ, respectively, where $\mathbf{e}^{\mathrm{n}}$ points outward. Additionally, $\mathbf{E}^{\infty}$ is the constant remote electric field, while jump brackets $[\![]\!]$ indicate the difference between the embraced quantity's limit values approaching from either domain, e.g.,

$$[\![\mathbf{E}]\!](\mathbf{x}^{\mathrm{e}}) = \lim_{\mathbf{x}^{\mathrm{o}} \to \mathbf{x}^{\mathrm{e}}} \mathbf{E}(\mathbf{x}^{\mathrm{o}}) - \lim_{\mathbf{x}^{\mathrm{i}} \to \mathbf{x}^{\mathrm{e}}} \mathbf{E}(\mathbf{x}^{\mathrm{i}}) , \quad \mathbf{x}^{\mathrm{o}} \in \Omega^{\mathrm{o}} , \mathbf{x}^{\mathrm{i}} \in \Omega^{\mathrm{i}} , \mathbf{x}^{\mathrm{e}} \in \Gamma . \tag{8}$$

For the sake of clarity, the fields are split with respect to the domains in terms of

$$\mathbf{E} = \begin{cases} \mathbf{E}^{\mathrm{o}} & \text{in } \Omega^{\mathrm{o}} \\ \mathbf{E}^{\mathrm{i}} & \text{in } \Omega^{\mathrm{i}} \end{cases} , \quad \mathbf{D} = \begin{cases} \mathbf{D}^{\mathrm{o}} & \text{in } \Omega^{\mathrm{o}} \\ \mathbf{D}^{\mathrm{i}} & \text{in } \Omega^{\mathrm{i}} \end{cases} , \tag{9}$$

where $\mathbf{E}^{\mathrm{o}}, \mathbf{D}^{\mathrm{o}} \in C^1(\overline{\Omega^{\mathrm{o}}}, \mathbb{R}^2)$ and $\mathbf{E}^{\mathrm{i}}, \mathbf{D}^{\mathrm{i}} \in C^1(\overline{\Omega^{\mathrm{i}}}, \mathbb{R}^2)$. Lastly, the problem outlined so far is depicted in Fig. 1. The solution is obtained in the style of [5, 6], who exploited holomorphic potentials of the complex variable $z = x_1 + \mathrm{i}x_2$ in the framework of complex analysis:

$$E_1(x_1, x_2) - \mathrm{i}E_2(x_1, x_2) = \begin{cases} C_{\mathrm{i}} , & \mathbf{x} \in \Omega^{\mathrm{i}} \\ \dfrac{\overline{E^{\infty}}(h(x_1 + \mathrm{i}x_2))^2 + C_{\mathrm{o}}}{(h(x_1 + \mathrm{i}x_2))^2 - m} , & \mathbf{x} \in \Omega^{\mathrm{o}} \end{cases} , \tag{10}$$

[2] the curl operator in this work is to be understood as its two-dimensional formulation, i.e., with $\mathbf{f} \in C^1(X \subseteq \mathbb{R}^2, \mathbb{R}^2)$ follows $\operatorname{curl} : C^1(X, \mathbb{R}^2) \to C(X, \mathbb{R})$, $\mathbf{f} \mapsto \operatorname{curl} \mathbf{f} = \frac{\partial f_2}{\partial x_1} - \frac{\partial f_1}{\partial x_2}$

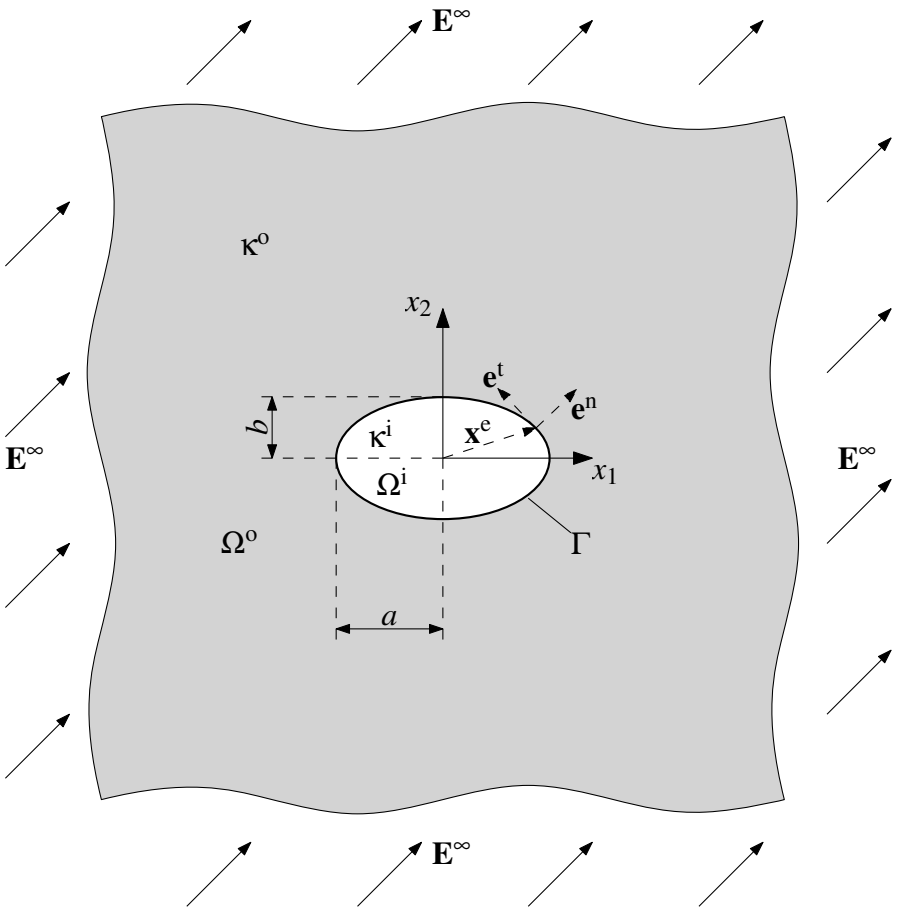

Figure 1: Illustration of the boundary value problem of an infinite dielectric with elliptic cavity subjected to remote electric loads.

as well as

$$\alpha(x_1,x_2)=\begin{cases}-C_{\mathrm{i}}R(h(x_1+\mathrm{i}x_2)+m(h(x_1+\mathrm{i}x_2))^{-1})\,, & \mathbf{x}\in\Omega^{\mathrm{i}}\\ R(-\overline{E^{\infty}}h(x_1+\mathrm{i}x_2)+C_{\mathrm{o}}(h(x_1+\mathrm{i}x_2))^{-1})\,, & \mathbf{x}\in\Omega^{\mathrm{o}}\end{cases}\,, \tag{11}$$

where $a=R(1+m), b=R(1-m)^3$ and $E^{\infty}=E_1^{\infty}+\mathrm{i}E_2^{\infty}$. The constants $C_{\mathrm{i}}, C_{\mathrm{o}}\in\mathbb{C}$ are given by

$$C_{\mathrm{i}}=\frac{2\kappa^{\mathrm{o}}[(\kappa^{\mathrm{o}}+\kappa^{\mathrm{i}})\overline{E^{\infty}}-m(\kappa^{\mathrm{o}}-\kappa^{\mathrm{i}})E^{\infty}]}{[\kappa^{\mathrm{o}}(1+m)+\kappa^{\mathrm{i}}(1-m)][\kappa^{\mathrm{o}}(1-m)+\kappa^{\mathrm{i}}(1+m)]}\,, \tag{12}$$

$$C_{\mathrm{o}}=\frac{[(\kappa^{\mathrm{i}})^2-(\kappa^{\mathrm{o}})^2][1-m^2]E^{\infty}-4m\kappa^{\mathrm{o}}\kappa^{\mathrm{i}}\overline{E^{\infty}}}{[\kappa^{\mathrm{o}}(1+m)+\kappa^{\mathrm{i}}(1-m)][\kappa^{\mathrm{o}}(1-m)+\kappa^{\mathrm{i}}(1+m)]}\,, \tag{13}$$

[3]With $R>0$ and $m\in[0,1)$, a slit crack is obtained for $m\to 1$.

and the function $h : \mathbb{C} \setminus [-2R\sqrt{m}, 2R\sqrt{m}] \to \mathbb{C} \setminus \overline{\mathbb{D}(\sqrt{m})}$ reads[4]

$$h(z) = \frac{1}{2R}\left(z + \sqrt{z + 2R\sqrt{m}}\sqrt{z - 2R\sqrt{m}}\right). \tag{14}$$

By means of Eq. (10) and (11), approximated surface charges and Coloumbic tractions are determined using Eqs. (1) and (2) with replacement of $u_2 \to x_2^{\mathrm{e}}$ with $\mathbf{x}^{\mathrm{e}} \in \Gamma$, both turning out constant on the upper as well as lower crack face, respectively, where the corresponding values are additive inverses of each other. Beyond that, the true surface charges ω_{S} and Maxwell surface tractions $\mathbf{t}^{\mathrm{M}}$ on Γ are calculated via

$$\omega_{\mathrm{S}} = \mathbf{e}^{\mathrm{n}} \cdot \mathbf{D}^{\mathrm{o}}\,, \tag{15}$$

$$\mathbf{t}^{\mathrm{M}} = \mathbf{e}^{\mathrm{n}} \cdot [\![\mathbf{T}]\!]\,, \tag{16}$$

with $\mathbf{T}$ as the Maxwell stress tensor according to Minkowski [7], which is given by

$$\mathbf{T} = \mathbf{D} \otimes \mathbf{E} - \frac{1}{2}(\mathbf{E} \cdot \mathbf{D})\mathbf{I}\,, \tag{17}$$

with $\mathbf{I}$ as the second-order unit tensor. In light of the following investigations, a parametrization $\mathbf{x}^{\mathrm{e}} : [0, 2\pi] \to \mathbb{R}^2$ of the ellipse Γ in terms of the parameter ϑ is introduced as

$$\mathbf{x}^{\mathrm{e}}(\vartheta) = R(1+m)\cos(\vartheta)\mathbf{e}_1 + R(1-m)\sin(\vartheta)\mathbf{e}_2\,, \tag{18}$$

so that we write, e.g., $\tilde{\omega}_{\mathrm{S}}(\vartheta) = \omega_{\mathrm{S}}(\mathbf{x}^{\mathrm{e}}(\vartheta))$ and $\tilde{\mathbf{t}}^{\mathrm{M}}(\vartheta) = \mathbf{t}^{\mathrm{M}}(\mathbf{x}^{\mathrm{e}}(\vartheta))$.

3 RESULTS

Let γ^{∞} denote the angle enclosed by the electric field $\mathbf{E}^{\infty}$ and the x_1-axis. The capacitor analogy's quality is illuminated in Fig. 2 for an inclined electric load, where the normalized surface charge $\tilde{\omega}_{\mathrm{S}}/|\tilde{\omega}_{\mathrm{S}}^{\mathrm{C}}|$[5] is plotted vs. the ratio $\kappa^{\mathrm{o}}/\kappa^{\mathrm{i}}$ for a pronounced ellipse with $m = 0.5$ in Fig. 2a and vs. the parameter m for a small ratio of $\kappa^{\mathrm{o}}/\kappa^{\mathrm{i}} = 10$ in Fig. 2b. The former brings out that the ratio $\tilde{\omega}_{\mathrm{S}}/|\tilde{\omega}_{\mathrm{S}}^{\mathrm{C}}|$ is insensitive to the quotient of permittivies, whereas the latter highlights the speed of convergence for $m \to 1$. Most notably, relative underestimations by $\omega_{\mathrm{S}}^{\mathrm{C}}$ are bounded by roughly 50%. In conclusion, enforcement of the surface charge density $\omega_{\mathrm{S}}^{\mathrm{C}}$ as electric Neumann boundary condition provides a good ersatz for the real electric interface conditions if $1 - m \ll 1$, independently of the ratio of permittivites $\kappa^{\mathrm{o}}/\kappa^{\mathrm{i}}$ and angle γ^{∞}.
On the other hand, at the example of barium titanate, Fig. 3 reveals drastic deviations of the Minkowski tractions t_1^{M} and t_2^{M} from the Coulombic one due to curvature when approaching the crack tip, where the former's magnitude succeeds the latter's by several orders. This owes to the field concentration $E_2^{\mathrm{o}}/E_2^{\infty}$ near the vertices for $m \to 1, m < 1$ tending to the factor $\kappa^{\mathrm{o}}/\kappa^{\mathrm{i}}$

[4] $\mathbb{D}(r) = \{z \in \mathbb{C} \mid z\overline{z} < r^2\}$ denotes the open disk of radius r centered at the origin.

[5] the quotient $\tilde{\omega}_{\mathrm{S}}/|\tilde{\omega}_{\mathrm{S}}^{\mathrm{C}}|$, by contrast to both of its constituents, depends on the permittivies only in terms of the ratio $\kappa^{\mathrm{o}}/\kappa^{\mathrm{i}}$.

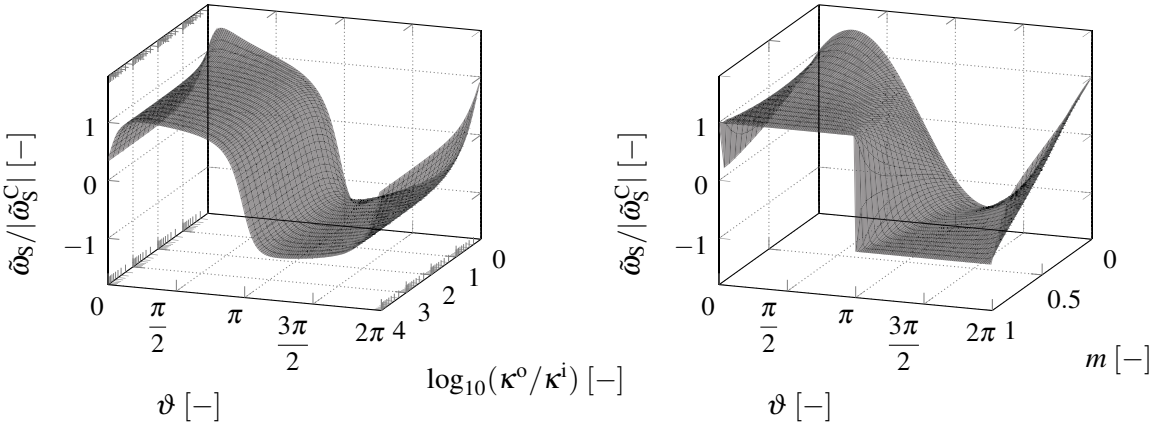

(a) $m = 0.5$ (b) $\kappa^\mathrm{o}/\kappa^\mathrm{i} = 10$

Figure 2: Infinite isotropic dielectric (κ^o) with elliptic cavity (κ^i) subjected to an oblique remote load $\mathbf{E}^\infty$ with $\gamma^\infty = \pi/4$: actual surface charge density $\tilde{\omega}_\mathrm{S}$ at the ellipse normalized with respect to the absolute value of the capacitor analogy $\tilde{\omega}_\mathrm{S}^\mathrm{C}$; (a): plotted vs. the common logarithm of the ratio $\kappa^\mathrm{o}/\kappa^\mathrm{i}$, (b): plotted vs. slenderness parameter m.

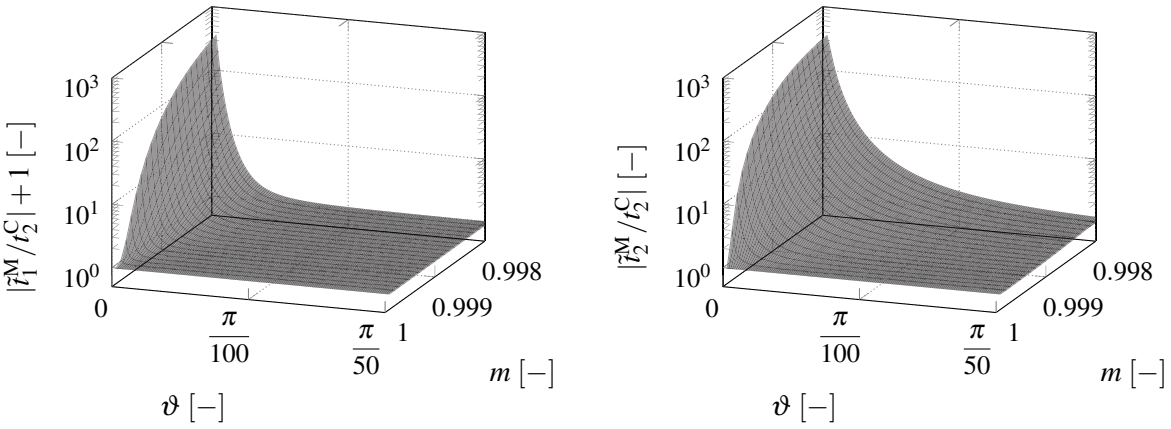

(a) (b)

Figure 3: Barium titanate exhibiting an elliptic cavity filled with vacuum ($m \leq 1, \kappa^\mathrm{i} = \kappa_0$) subjected to oblique remote load $\mathbf{E}^\infty$ with $|\mathbf{E}^\infty| = 2\,\mathrm{kV/mm}$ and $\gamma^\infty = \pi/4$; absolute value of (a): the Maxwell traction $\tilde{t}_1^\mathrm{M}$, and (b): $\tilde{t}_2^\mathrm{M}$, normalized with respect to the Coulombic traction $\tilde{t}_2^\mathrm{C}$ vs. slenderness parameter m.

[8], which amounts to roughly 1300 for barium titanate [9]. However, these large errors are constricted to the immediate neighbourhood of the vertices, which begs the question whether or not they are relevant for crack tip loading of opened cracks. For this purpose, consider a Griffith crack in an isotropic linear-elastic and dielectric material in plane strain subjected to

loads at infinity in terms of the tensile stress σ_{22}^{∞} and the electric displacement $\mathbf{D}^{\infty} = \kappa^{\mathrm{o}}\mathbf{E}^{\infty}$. The mechanical load will distort the crack into an elliptic shape with parameters [10]

$$R(\sigma_{22}^{\infty}) = \frac{1}{4}\left(1 + \frac{1-\nu}{2\mu}\sigma_{22}^{\infty}\right) l\,, \tag{19}$$

$$m(\sigma_{22}^{\infty}) = \frac{1 - \dfrac{3(1-\nu)}{2\mu}\sigma_{22}^{\infty}}{1 + \dfrac{1-\nu}{2\mu}\sigma_{22}^{\infty}}\,, \tag{20}$$

where ν and μ are Poisson's ratio and the shear modulus, respectively. After surface charges and Maxwell tractions are calculated in this deformed configuration, they are finally employed as boundary conditions on the crack faces in the undeformed configuration of the same body, for which we wish to determine the intensity factors $K_I = K_I^{\infty} + K_I^{\mathrm{cf}}$ and $K_{IV} = K_{IV}^{\infty} + K_{IV}^{\mathrm{cf}}$ due to the combined loading at infinity (superscript ∞) and at the crack faces (superscript cf) [6]. This issue is addressed with the aid of crack weight functions, which allow for the calculation of intensity factors for arbitrarily loaded crack faces based on the known solutions of references problems [12, 13]. Exploiting the reference solution of a Griffith crack loaded at infinity in terms of σ_{22}^{∞} and D_2^{∞} with traction and charge free crack faces, the desired intensity factors K_{IV} and K_I are computed analytically and numerically, respectively. The former turns out not to depend on D_1^{∞} and is depicted in Fig. 4, where in Fig. 4a, the three distinct crack conditions with regard to electric permeability well-known in literature [14] are to be differentiated:

- permeable crack: $K_{IV}/(\sqrt{\pi a} D_2^{\infty}) = 0$ for $\kappa^{\mathrm{o}}/\kappa^{\mathrm{i}} > 0$ and $\sigma_{22}^{\infty} = 0\,,$
- semi-permeable crack: $K_{IV}/(\sqrt{\pi a} D_2^{\infty}) \in (0,1)$ for $\kappa^{\mathrm{o}}/\kappa^{\mathrm{i}} > 0$ and $\sigma_{22}^{\infty} > 0\,,$
- impermeable crack: $K_{IV}/(\sqrt{\pi a} D_2^{\infty}) = 1$ for $\kappa^{\mathrm{o}}/\kappa^{\mathrm{i}} \to \infty$ and $\sigma_{22}^{\infty} \geq 0\,.$

To begin with, K_{IV} equals zero for a closed, permeable crack and rises for increasing σ_{22}^{∞} and $\kappa^{\mathrm{o}}/\kappa^{\mathrm{i}}$, reflecting the semi-permeable nature of an opened crack. Ultimately, for $\kappa^{\mathrm{i}} = 0$ or $\kappa^{\mathrm{o}} \to \infty$, impermeable conditions are recovered. The quality of the capacitor analogy, on the other hand, can be extracted from Fig. 4b, where for $\sigma_{22}^{\infty} > 0$, K_{IV}^{C} slightly overestimates K_{IV}^{cf}. However, for relevant stresses of up to $50\,\mathrm{MPa}$, the deviation amounts to less than a thousandth, rendering the differences between K_{IV}^{cf} and K_{IV}^{C} negligible.
Furthermore, with respect to K_I, vacuum and barium titanate are chosen as inner and outer dielectric, respectively, with the results for variable γ^{∞} and σ_{22}^{∞} visualized in Fig. 5 for an inclined load with $|\mathbf{E}^{\infty}| = 2\,\mathrm{kV/mm}$. Firstly, in Fig. 5a, the stress $\sigma_{22}^{\mathrm{cf}}$ corresponding to the intensity factor $K_I^{\mathrm{cf}} = \sqrt{\pi a}\sigma_{22}^{\mathrm{cf}}$ is plotted. It can be observed that the magnitude of $\sigma_{22}^{\mathrm{cf}}$ reaches up to $30\,\mathrm{MPa}$ for vertical electric loads in the case of a closed crack, i.e., $\sigma_{22}^{\infty} = 0$. Upon opening of the crack, $\sigma_{22}^{\mathrm{cf}}$ generally decreases, thus reducing the crack closing effect of the

[6] A similar procedure is described in [11], where the impact of Maxwell tractions on a conducting crack in an infinite dielectric is investigated.

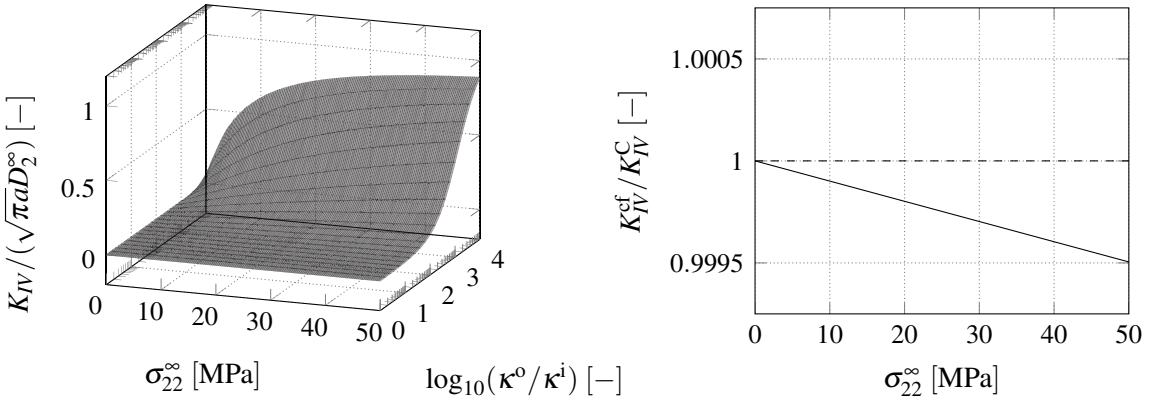

(a) (b)

Figure 4: Illustration of electric intensity factors: (a): total factor $K_{IV} = K_{IV}^{\infty} + K_{IV}^{\mathrm{cf}}$ normalized with respect to $K_{IV}^{\infty} = \sqrt{\pi a} D_2^{\infty}$ as function of stress load dependent slenderness parameter $m(\sigma_{22}^{\infty})$ plotted vs. σ_{22}^{∞} and the common logarithm of the ratio $\kappa^{\mathrm{o}}/\kappa^{\mathrm{i}}$, (b): quotient K_{IV}^{cf} due to true crack face charges ω_{S} as function of $m(\sigma_{22}^{\infty})$ and K_{IV}^{C} due to crack face charges $\omega_{\mathrm{S}}^{\mathrm{C}}$ according to the capacitor analogy.

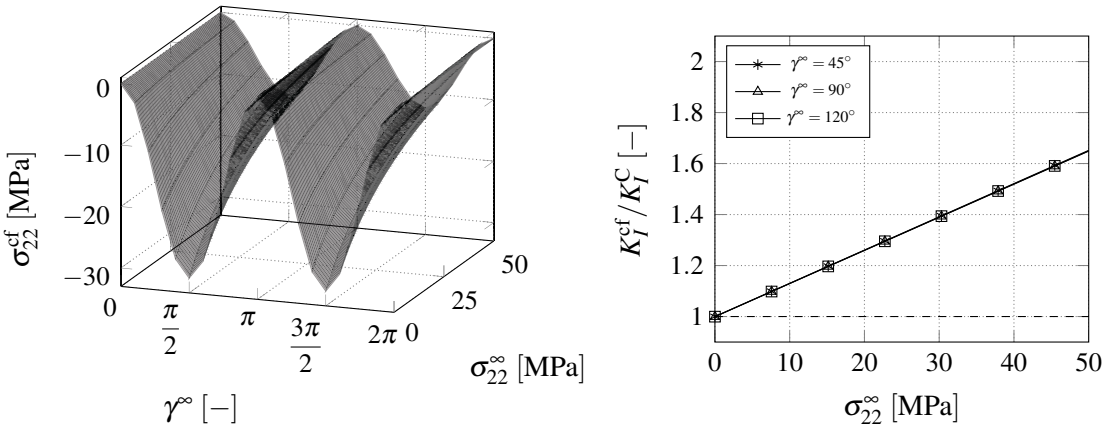

(a) (b)

Figure 5: Depiction of mechanical stress intensity factors for barium titanate with $|\mathbf{E}^{\infty}| = 2\,\mathrm{kV/mm}$, (a): stress $\sigma_{22}^{\mathrm{cf}}$ due to Maxwell tractions t_2^{M} as function of stress load dependent slenderness parameter $m(\sigma_{22}^{\infty})$ plotted vs. σ_{22}^{∞} and angle of the electric load γ^{∞}; (b) ratio of true and approximated intensity factors $K_I^{\mathrm{cf}}/K_I^{\mathrm{C}}$ vs. σ_{22}^{∞} for elected angles γ^{∞}.

Maxwell tractions. It is particularly worth noting that K_I^{C} significantly underestimates the true factor K_I^{cf} as depicted in Fig. 5b. While both factors are nearly identical for a closed crack, their deviation increases independently of the angle γ^{∞} and well-nigh linearly with the applied load,

amounting to more than $60\,\%$ for $\sigma_{22}^{\infty} = 50\,\mathrm{MPa}$. Consequently, the enormous concentration of traction near the crack tip shown in Fig. 3b, although restricted to a tiny portion of the crack faces, reflects in a distinctly larger intensity factor compared with uniform loading.

4 CONCLUSIONS

The capacitor analogy provides crack face conditions in terms of approximate surface charges $\omega_{\mathrm{S}}^{\mathrm{C}}$ and Coulombic tractions t_2^{C} accounting for an opened crack. By considering the closed-form solution of an elliptic cavity in an infinite dielectric, the quality of these approximate quantities could be evaluated, revealing that, although the crack's curvature is neglected, surface charges $\omega_{\mathrm{S}}^{\mathrm{C}}$ are calculated within a marginal range of deviation from the true charges ω_{S}. Thus, the mode IV intensity factor K_{IV}^{C} poses an excellent substitute for the real factor K_{IV}^{cf}. The Coulombic tractions, however, fail to properly embody the true tractions $\mathbf{t}^{\mathrm{M}}$ close to the crack tips where orders of magnitude of relative errors amount up to 10^2. As a consequence, the mode I stress intensity factor K_I^{C} significantly underestimates the true factor K_I^{cf}, thus resulting in an incorrectly small closening effect. In conclusion, crack curvature has to be accounted for in order to appropriately capture the influence of Maxwell tractions at dielectric crack faces.

REFERENCES

[1] T.-H. Hao and Z.-Y. Shen, "A new electric boundary condition of electric fracture mechanics and its applications," *Engineering Fracture Mechanics*, vol. 47, no. 6, pp. 793–802. [Online]. Available: https://linkinghub.elsevier.com/retrieve/pii/0013794494900590

[2] C. M. Landis, "Energetically consistent boundary conditions for electromechanical fracture," *International Journal of Solids and Structures*, vol. 41, no. 22, pp. 6291–6315. [Online]. Available: https://linkinghub.elsevier.com/retrieve/pii/S0020768304002987

[3] A. Ricoeur and M. Kuna, "Electrostatic tractions at dielectric interfaces and their implication for crack boundary conditions," *Mechanics Research Communications*, vol. 36, no. 3, pp. 330–335. [Online]. Available: https://linkinghub.elsevier.com/retrieve/pii/S0093641308001304

[4] A. Ricoeur, R. Gellmann, and Z. Wang, "Influence of inclined electric fields on the effective fracture toughness of piezoelectric ceramics," *Acta Mechanica*, vol. 226, no. 2, pp. 491–503. [Online]. Available: http://link.springer.com/10.1007/s00707-014-1190-5

[5] R. J. Knops, "Two-dimensional electrostriction," *The Quarterly Journal of Mechanics and Applied Mathematics*, vol. 16, no. 3, pp. 377–388. [Online]. Available: https://academic.oup.com/qjmam/article-lookup/doi/10.1093/qjmam/16.3.377

[6] T. E. Smith and W. E. Warren, "Some problems in two-dimensional electrostriction," *Journal of Mathematics and Physics*, vol. 45, no. 1, pp. 45–51. [Online]. Available: https://onlinelibrary.wiley.com/doi/10.1002/sapm196645145

[7] V. V. Datsyuk and O. R. Pavlyniuk, “Maxwell stress on a small dielectric sphere in a dielectric,” *Physical Review A*, vol. 91, no. 2. [Online]. Available: https://link.aps.org/doi/10.1103/PhysRevA.91.023826

[8] R. M. McMeeking, “Electrostrictive stresses near crack-like flaws,” *ZAMP Journal of Applied Mathematics and Physics*, vol. 40, no. 5, pp. 615–627. [Online]. Available: http://link.springer.com/10.1007/BF00945867

[9] S. B. Deshpande, P. D. Godbole, Y. B. Khollam, and H. S. Potdar, “Characterization of barium titanate: BaTiO3 (BT) ceramics prepared from sol-gel derived BT powders,” *Journal of Electroceramics*, vol. 15, no. 2, pp. 103–108. [Online]. Available: http://link.springer.com/10.1007/s10832-005-1460-7

[10] M. Kuna, *Finite Elements in Fracture Mechanics: Theory - Numerics - Applications*, ser. Solid Mechanics and Its Applications. Springer Netherlands, vol. 201. [Online]. Available: https://link.springer.com/10.1007/978-94-007-6680-8

[11] R. M. McMeeking, “On mechanical stresses at cracks in dielectrics with application to dielectric breakdown,” *Journal of Applied Physics*, vol. 62, no. 8, pp. 3116–3122. [Online]. Available: http://aip.scitation.org/doi/10.1063/1.339361

[12] R. McMeeking and A. Ricoeur, “The weight function for cracks in piezoelectrics,” *International Journal of Solids and Structures*, vol. 40, no. 22, pp. 6143–6162. [Online]. Available: https://linkinghub.elsevier.com/retrieve/pii/S0020768303003664

[13] K. Wippler, A. Ricoeur, and M. Kuna, “Towards the computation of electrically permeable cracks in piezoelectrics,” *Engineering Fracture Mechanics*, vol. 71, no. 18, pp. 2567–2587. [Online]. Available: https://linkinghub.elsevier.com/retrieve/pii/S0013794404000761

[14] M. Kuna, “Fracture mechanics of piezoelectric materials – where are we right now?” *Engineering Fracture Mechanics*, vol. 77, no. 2, pp. 309–326. [Online]. Available: https://linkinghub.elsevier.com/retrieve/pii/S0013794409000939